

## Role of hydrogen and lithium impurities in radiation damage in neutron-irradiated MgO single crystals

R. González, I. Vergara, and D. Cáceres

*Departamento de Física, Escuela Politécnica Superior, Universidad Carlos III, Avda. de la Universidad, 30, 28911 Leganés, (Madrid), Spain*

Y. Chen

*Division of Materials Sciences, Office of Basic Energy Sciences, SC 13, The U.S. Department of Energy, Germantown, Maryland 20874-1290*

(Received 29 January 2002; revised manuscript received 20 March 2002; published 6 June 2002)

Radiation damage induced by neutron irradiation was studied by optical absorption measurements in undoped MgO crystals and in MgO crystals intentionally doped with either hydrogen or lithium impurities. The oxygen-vacancy concentration incurred by the neutron irradiation increases with neutron dose. Suppression of radiation damage as characterized by oxygen vacancies is observed in MgO:H crystals and attributed to migration of oxygen vacancies to microcavities filled with hydrogen gas. In MgO:Li crystals irradiated with neutron doses below  $10^{18}$  neutrons/cm<sup>2</sup>, most of the oxygen vacancies are camouflaged as hydride ions formed by the capture of protons by the oxygen vacancies. Substitutional lithium ions are also displaced. We postulate that they aggregate at Li<sub>2</sub>O precipitates. Thermal annealing experiments demonstrate that protons are mobile at 700 K and lithium ions at 1100 K.

DOI: 10.1103/PhysRevB.65.224108

PACS number(s): 61.72.Ji, 62.20.Qp, 62.20.Dc

### I. INTRODUCTION

The irradiation of MgO single crystals by energetic neutrons ( $E > 0.1$  MeV) produces<sup>1</sup> several optically detectable defects: (1) anion vacancies (primarily the one-electron  $F^+$  center) which absorb at about 250 nm (5.0 eV),<sup>2,3</sup> (2) anion divacancies,  $F_2$ , which absorb at 355 and 975 nm (3.49 and 1.27 eV, respectively),<sup>4-7</sup> and (3) an unidentified higher-order point defect which absorbs at 573 nm (2.16 eV).<sup>2,7-10</sup> Cation vacancies are produced, but they do not survive, because the cation interstitials are unstable and quickly recombine with the vacancies. Cation vacancies can be produced by the displacement of protons substituting for magnesium ions via an ionization mechanism<sup>11,12</sup>; however, this will not be discussed here.

Impurity ions play important roles in the rate of production of radiation-induced defects in crystalline solids. In general, impurities enhance the production rate of surviving vacancies, because displaced interstitials are trapped by the impurities.<sup>13</sup> In MgO, the formation of  $F^+$  centers is enhanced by the presence of Fe impurities.<sup>13</sup> However, when doped individually with two light impurities, MgO crystals exhibit a decrease in vacancy concentrations. In nominally pure MgO crystals annealed at high temperature in hydrogen prior to reactor irradiation, the vacancy concentration at saturation doses is only about 70% of that recorded in unannealed crystals.<sup>14</sup> It has been proposed that the decrease results from the migration of vacancies to macroscopic voids, formed by a preirradiation annealing treatment. When doped with a concentration of  $2 \times 10^{19}$  cm<sup>-3</sup> lithium ions,<sup>15</sup> a reduced concentration of  $F^+$  and  $F_2$  centers has been observed. A satisfactory explanation of the role played by the lithium ions has not yet been provided.

The mechanisms for displacement are the same in both

doped and undoped crystals, but the concentration of *surviving* defects depends on the crystal impurity content. The purpose of the present paper is to elucidate the role played by these two light ion impurities in reducing the concentrations of defects, such as  $F^+$  centers. This work is divided into four sections. The first section addresses the formation of  $F^+$  centers in nominally pure MgO single crystals. In the second section, neutron irradiation of crystals containing large concentrations of hydrogen is investigated. The third section concerns the inhibition of  $F^+$  centers in lithium-doped MgO crystals. The fourth section analyzes the isochronal annealing behavior of neutron-irradiated MgO:Li crystals.

### II. EXPERIMENTAL PROCEDURE

The single crystals of magnesium oxide used in this investigation were grown at the Oak Ridge National Laboratory by an arc-fusion technique using high-purity MgO powder from Kanto Chemical Chemistry, Tokyo, Japan.<sup>16</sup> Typical chemical analyses have been reported previously.<sup>16,17</sup> MgO crystals intentionally doped with hydrogen were produced by presoaking the starting MgO powder with water. The resulting crystals were very cloudy due to the presence of cavities containing high-pressure hydrogen gas.<sup>18,19</sup> Lithium doping was achieved by mixing 5% of Li<sub>2</sub>CO<sub>3</sub> powder with MgO powder before crystal growth. The actual lithium concentration in the resulting single crystals was determined by spectrographic analysis to be 400 ppm.

Neutron irradiations were performed either at the Oak Ridge National Laboratory Low Temperature Neutron Irradiation Facility or at the High Flux Reactor of the Institute for Advanced Materials of the Joint Research Center (JRC) at Petten. The fluxes were  $2.0 \times 10^{17}$  and  $7.8 \times 10^{17}$  fission spectrum neutrons/(cm<sup>2</sup> s) ( $E > 0.1$  MeV), respectively. The ambient temperature in both cases was  $325 \pm 20$  K.

TABLE I. Conversion factors from absorption coefficient ( $\alpha$ ) to defect concentration ( $n$ ),  $n=C\alpha$ , for  $F^+$ ,  $[H^-]^+$ , and  $V_{OH}^-$  centers.

Defect	Defect description	$C(\text{cm}^{-2})$
$F^+$	Oxygen vacancy which has trapped an electron	$5 \times 10^{15}$
$[H^-]^+$	Oxygen vacancy occupied by a proton	$5.5 \times 10^{16}$
$V_{OH}^-$	A proton substituting for a $\text{Mg}^{2+}$ ion	$3 \times 10^{16}$

Optical absorption measurements in the UV-VIS-IR regions were made with a Perkin-Elmer Lambda 19 spectrophotometer. Far-infrared data were taken with a Perkin-Elmer FT-IR 2000 spectrophotometer. Heat treatments were made in flowing high-purity nitrogen gas inside a horizontal furnace.

### III. EXPERIMENTAL RESULTS

In MgO crystals, elastic collisions of energetic neutrons with lattice ions can produce anion vacancies with one and two electrons:  $F^+$  and  $F$  centers, respectively. In neutron-irradiated crystals the anion vacancies prefer to be in the  $F^+$  state. The absorption coefficient of the band at 5.0 eV is a reliable determination of the anion-vacancy concentration, regardless of the charge state. Both the neutral  $F$  center and the positively charged  $F^+$  absorb at this energy. The  $F$  center absorbs at 5.01 eV, and the  $F^+$  center at 4.92 eV.<sup>2,3</sup> Although the oscillator strengths and full widths at half maximum (FWHM) of these centers are different, their values compensate one another in such a way that the measurement of the absorption coefficient at this energy conveniently determines the sum of the concentrations of both centers. The conversion factor from absorption coefficient to concentration is  $5 \times 10^{15} \text{ cm}^{-2}$ .<sup>13</sup> In heavily irradiated crystals, the absorption coefficients were obtained by determining the wavelength at which the half-maximum absorption occurs. Table I summarizes the conversion factors from absorption coefficient to defect concentration for various defects in MgO crystals.

#### A. Nominally pure MgO crystals

In Fig. 1, the  $F^+$  concentrations of the neutron-irradiated crystals are plotted versus neutron doses on a log-log plot. The concentration of anion vacancies increases with neutron dose, in agreement with previous findings.<sup>7,20</sup>

In an early work on samples with different iron concentrations, it was observed that higher Fe content results in higher  $F^+$  concentration under either neutron or electron irradiation.<sup>13</sup> The increased damage in crystals with a larger impurity concentration has been associated with the trapping of displaced interstitials by impurities, thus preventing their recombination with vacancies. Interstitials wander into the neighborhood of an impurity atom and form an association with some binding energy due to lattice strains around the impurity.<sup>13</sup> In general, more impurities mean more trapped interstitials and as a result more surviving vacancies. However, vacancy concentrations can be diminished by doping

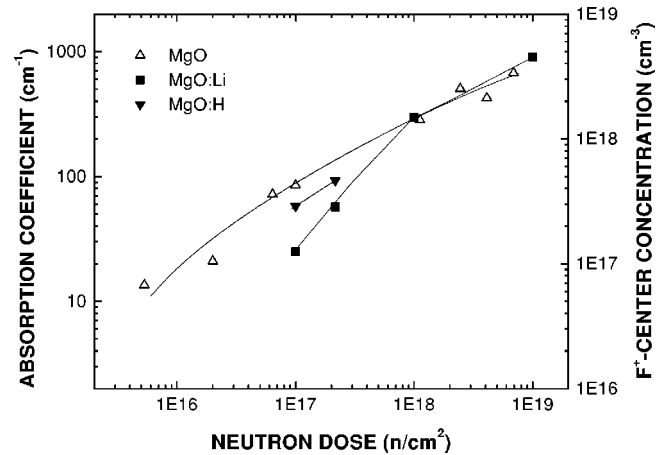


FIG. 1. Log-log plot of the absorption coefficient at the peak of the 5.0 eV band vs neutron dose for undoped MgO, MgO:H, and MgO:Li crystals. The ordinate on the right-hand side of the figure shows the corresponding  $F^+$ -center concentrations.

with selected impurities. In the next two sections, we shall present results in crystals intentionally doped with hydrogen or lithium.

#### B. Hydrogen-doped MgO crystals

In a previous study by Henderson *et al.*,<sup>14</sup> when nominally pure MgO crystals were subjected to irradiation with  $10^{19}$  neutrons/cm<sup>2</sup> after annealing in hydrogen at elevated temperatures, the concentration of  $F^+$  centers was reported to be 30% smaller than in unannealed samples. The reduced concentration was attributed to the migration of vacancies to large lenticular voids filled with hydrogen gas, induced by the preirradiation annealing treatment. In the present study, instead of preannealing in hydrogen, very cloudy MgO:H crystals were grown by presoaking the starting MgO powder in water. The opacity of the crystals is due to a very high concentration of cavities with an average size of 0.6  $\mu\text{m}$  filled with high-pressure hydrogen gas.<sup>19</sup> Two intense infrared bands appear at 3700  $\text{cm}^{-1}$  and 3296  $\text{cm}^{-1}$ . The 3700  $\text{cm}^{-1}$  band is due to  $\text{OH}^-$  ions in  $\text{Mg}(\text{OH})_2$  precipitates. The 3296  $\text{cm}^{-1}$  band can be regarded simply as a  $\text{H}^+$  substituting for a  $\text{Mg}^{2+}$  ion, with a linear configuration of  $\text{OH}^- [++]\text{O}^{2-}$ , where  $[++]$  refers to a  $\text{Mg}^{2+}$  vacancy.<sup>21,22</sup> This defect is therefore negatively charged with respect to its surrounding, and is commonly referred to as a  $V_{OH}^-$  center. To study the influence of this large hydrogen concentration on the production of  $F^+$  centers, the optical spectra of these cloudy crystals were compared with clear crystals after neutron irradiation with  $1.0 \times 10^{17}$  and  $2.0 \times 10^{17}$  neutrons/cm<sup>2</sup>. These crystals were all grown at the Oak Ridge National Laboratory.

Figure 2 shows the optical absorption spectra of a nominally pure MgO and a cloudy MgO:H sample, both irradiated to a dose of  $1.0 \times 10^{17}$  neutrons/cm<sup>2</sup>. Apart from an increase in the absorption of the base line of the MgO:H sample, which is more pronounced at higher energies due to light scattering from the cavities, the most noticeable difference between these two spectra occurs in the absorption at 5.0 eV,

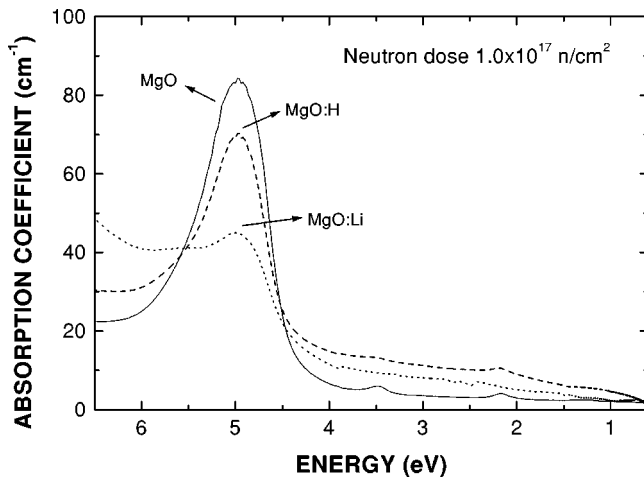


FIG. 2. Optical absorption spectra of undoped MgO, MgO:H, and MgO:Li after neutron irradiation to a dose of  $1.0 \times 10^{17}$  neutrons/cm<sup>2</sup>.

which is smaller for the MgO:H sample. The anion-vacancy concentrations in two MgO:H samples are plotted in Fig. 1. Relative to MgO, they were about 35% lower. These results confirm that the presence of microcavities containing hydrogen diminishes the net production of anion vacancies.

In the far-infrared region between 4000 and 1000 cm<sup>-1</sup> (not shown in Fig. 2), the only change after neutron irradiation was an increase of the 3700 cm<sup>-1</sup> band at the expense of the 3296 cm<sup>-1</sup> band. The relocation of protons was induced by the concomitant  $\gamma$  rays during neutron irradiation, which give rise to Compton electrons. These ionizing electrons displace protons from the  $V_{OH}^-$  centers to form Mg(OH)<sub>2</sub> precipitates, by a process termed radiation-induced diffusion (RID) with a phenomenally large cross section of about  $10^8$  b (where  $1 \text{ b} = 10^{-24} \text{ cm}^2$ ).<sup>12</sup>

### C. Lithium-doped MgO crystals

In a previous work by Chen and Abraham,<sup>15</sup> the net production of stable  $F^+$  centers has been shown to be suppressed about 50% by doping with  $\sim 2 \times 10^{19} \text{ cm}^{-3}$  lithium impurities. An explanation has not been provided. In order to identify the parameters responsible for this effect, four MgO:Li crystals were neutron irradiated with the following doses:  $1.0 \times 10^{17}$ ,  $2.0 \times 10^{17}$ ,  $1.0 \times 10^{18}$ , and  $1.0 \times 10^{19}$  neutrons/cm<sup>2</sup>.

The optical absorption spectrum of a MgO:Li sample after neutron irradiation with a dose of  $1.0 \times 10^{17}$  neutrons/cm<sup>2</sup> is also shown in Fig. 2. The most striking difference between this spectrum and that of the undoped crystal is the much lower absorption at 5.0 eV in the MgO:Li sample, which indicates an anion-vacancy concentration about 70% smaller, in good agreement with previous findings.<sup>15</sup> The absorption coefficients at 5.0 eV for the four neutron-irradiated MgO:Li samples are plotted as a function of dose in Fig. 1. The suppression of  $F^+$ -center production diminishes as the neutron dose increases. Above  $10^{18}$  neutrons/cm<sup>2</sup> it is nonexistent.

We shall now address the causes for the suppression of radiation damage in MgO:Li crystals at doses below  $10^{18}$

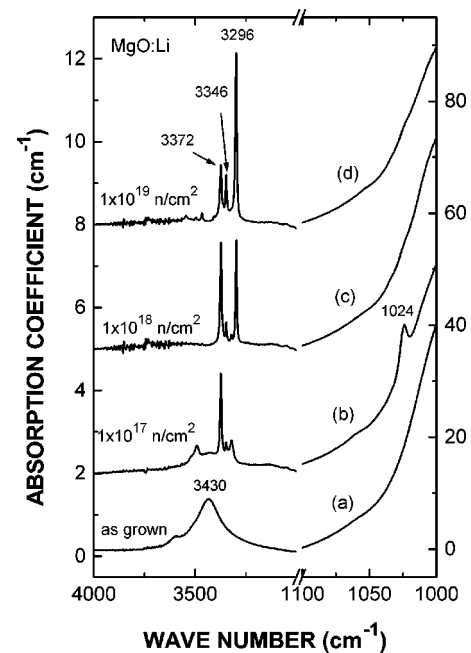


FIG. 3. Infrared optical absorption spectra of (a) an as-grown MgO:Li crystal and three MgO:Li crystals neutron irradiated to doses of (b)  $1.0 \times 10^{17}$ , (c)  $1.0 \times 10^{18}$ , and (d)  $1.0 \times 10^{19}$  neutrons/cm<sup>2</sup>, respectively.

neutrons/cm<sup>2</sup> and the absence of suppression at higher doses. There are two reasons. The first, already addressed above, is due to defect sinks at microcavities filled with hydrogen gas, with an average size of  $0.4 \mu\text{m}$ . These microcavities were observed by transmission electron microscopy in MgO:Li crystals.<sup>19</sup> However, microcavities alone can account for only a small portion of the inhibition of anion-vacancy formation. Their concentration in MgO:Li crystals is much smaller than in MgO:H. Therefore we conclude that the influence of cavities on anion-vacancy suppression is small.

A major reason for the loss of oxygen vacancies is that these vacancies had captured protons and were camouflaged as hydride ions  $[H^-]^+$  centers<sup>23,24</sup> (an oxygen vacancy occupied by a proton and therefore positively charged relative to the lattice). Indeed, three infrared bands<sup>23</sup> at 1024, 1032, and 1053 cm<sup>-1</sup>, associated with  $[H^-]^+$  centers, were observed. MgO:Li crystals have a strong affinity for hydrogen.<sup>24-26</sup> In the as-grown state, MgO:Li crystals exhibit a very broad IR band at 3430 cm<sup>-1</sup> associated with OH<sup>-</sup> complexes perturbed by Li<sup>+</sup> ions.<sup>24-26</sup> The sharp lines at 3296 cm<sup>-1</sup> and 3700 cm<sup>-1</sup>, which represent the most common stretching frequencies observed in lithium-free hydrogen-containing crystals, were absent.

Figure 3 shows the IR spectra for an as-grown MgO:Li crystal and for three MgO:Li samples that were neutron-irradiated to different doses. In the OH<sup>-</sup> region, the irradiation produced a dramatic decrease in a broadband absorption at 3430 cm<sup>-1</sup> with neutron dose. Sharp bands at 3372, 3346, 3320, and 3296 cm<sup>-1</sup> emerged. These bands are present, to a greater or lesser extent, in virtually all as-grown MgO crystals, except MgO:Li.<sup>21</sup> The 3296 cm<sup>-1</sup> band is due to the  $V_{OH}^-$  centers as noted, and the others are due to

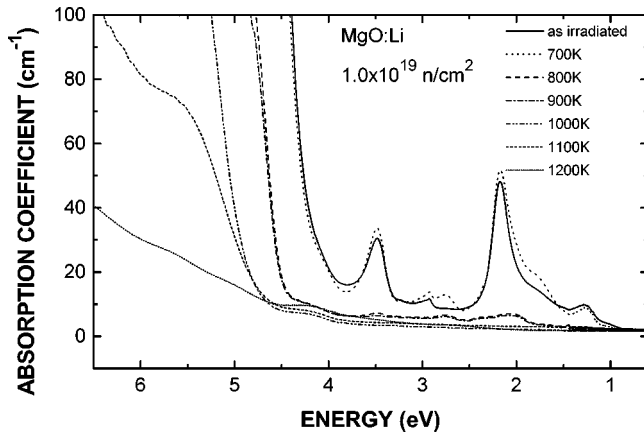


FIG. 4. Optical absorption spectra of an MgO:Li crystal neutron irradiated to a dose of  $1.0 \times 10^{19}$  neutrons/cm<sup>2</sup> and after isochronal annealing for 15 min at several selected temperatures.

OH<sup>-</sup> ions perturbed by nearby impurities. In contrast with other MgO crystals, the 3700 cm<sup>-1</sup> band was absent, before and after neutron irradiation. Furthermore, while the 3700 cm<sup>-1</sup> band is common to MgO crystals in general, it has not been observed in Li-doped crystals. Under irradiation, protons associated with substitutional Li<sup>+</sup> ions, characterized by the broad OH<sup>-</sup> band at 3430 cm<sup>-1</sup>, were displaced, resulting in OH<sup>-</sup> ions unperturbed by Li<sup>+</sup> ions, as illustrated by the sharp OH<sup>-</sup> bands. In spite of the smaller<sup>24</sup> ( $10^5$  b) but yet enormously large cross section, substitutional Li<sup>+</sup> ions would also be displaced. A question arises: where do these displaced Li<sup>+</sup> ions relocate?

As a result of the irradiation with a low dose of  $1.0 \times 10^{17}$  neutrons/cm<sup>2</sup>, an absorption band at 1024 cm<sup>-1</sup> is observed [Fig. 3(b)], which corresponds<sup>27</sup> to  $3.5 \times 10^{17}$  cm<sup>-3</sup> [H<sup>-</sup>]<sup>+</sup> centers. (The conversion factor is given in Table I.) Protons are readily relocated at oxygen vacancies, thereby creating [H<sup>-</sup>]<sup>+</sup> centers.<sup>23,27</sup> The oxygen vacancies in MgO and MgO:Li, irradiated to a dose of  $1.0 \times 10^{17}$  neutrons/cm<sup>2</sup>, are  $\sim 4.3 \times 10^{17}$  and  $1.3 \times 10^{17}$  cm<sup>-3</sup>, respectively. The discrepancy between these concentrations approximates the [H<sup>-</sup>]<sup>+</sup>-center concentration determined in the MgO:Li crystals. These results clearly show that in MgO:Li crystals, irradiated with  $1.0 \times 10^{17}$  neutrons/cm<sup>2</sup>, a substantial fraction of the oxygen vacancies are camouflaged as [H<sup>-</sup>]<sup>+</sup> centers. In the crystals irradiated to doses above  $1.0 \times 10^{18}$  neutrons/cm<sup>2</sup>, the concentration of [H<sup>-</sup>]<sup>+</sup> centers becomes very small and the F<sup>+</sup> concentration approximates that of undoped crystals (Fig. 1).

#### D. Radiation-damage recovery in neutron-irradiated MgO:Li crystals

An MgO:Li sample irradiated to a dose of  $1.0 \times 10^{19}$  neutrons/cm<sup>2</sup> was isochronally annealed at increasing temperatures above 500 K in flowing nitrogen gas. After each anneal, vacancy defects were characterized using UV-Visible-IR measurements (Fig. 4) and hydrogen-related defects using far-infrared spectroscopy (Fig. 5). The spectra in Fig. 4 show that at 700 K a slight decrease in anion-vacancy

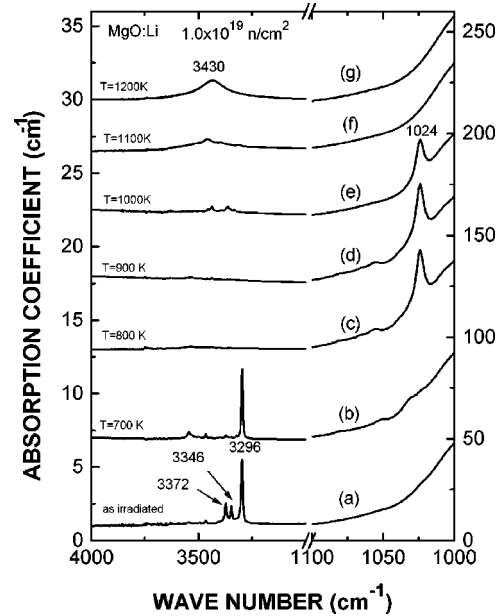


FIG. 5. Infrared optical absorption spectra of the same MgO:Li crystal used in Fig. 4.

concentration (5.0 eV band) was attended by a small increase in the concentrations of divacancies (3.49 and 1.27 eV bands) and other higher-order point defects involving oxygen vacancies (2.94, 2.75 and 2.16 eV bands). Since vacancies are not mobile at this temperature,<sup>27</sup> the change in vacancy concentrations is attributed to valence change. In the far-infrared region, the protons were mostly in OH<sup>-</sup> sites, but the [H<sup>-</sup>]<sup>+</sup> bands at 1024, 1032, and 1053 cm<sup>-1</sup> began to emerge [Fig. 5(b)]. Protons from OH<sup>-</sup> sites began to be mobile, resulting in the occupation of anion vacancies.

Annealing at 800 K, the anion-vacancy and higher-order vacancy concentrations diminished dramatically (Fig. 4). The OH<sup>-</sup> bands virtually disappeared and the [H<sup>-</sup>]<sup>+</sup> centers were formed [Fig. 5(c)]. However, the estimated  $1.5 \times 10^{17}$  cm<sup>-3</sup> protons lost from OH<sup>-</sup> ions were insufficient to form  $\sim 2 \times 10^{18}$  cm<sup>-3</sup> [H<sup>-</sup>]<sup>+</sup> centers. (The conversion factor reported in Ref. 18 is given in Table I.) We conjecture that most of the protons came from the hydrogen gas in the microcavities. With further annealing at 900 K, the 5.0 eV band continued to diminish, while the [H<sup>-</sup>]<sup>+</sup> centers remained unchanged [Fig. 5(d)].

Annealing at 1000 K depleted all anion vacancies, but the sharp band at 1024 cm<sup>-1</sup> decayed only slightly [Fig. 5(e)]. A previous study indicated that in a thermochemically reduced MgO crystal, in which anion vacancies are created nonstoichiometrically at 2400 K in Mg vapor, anion vacancies are less stable than those occupied by protons.<sup>24</sup> Likewise in a neutron-irradiated crystal, we demonstrated here that the presence of a proton stabilizes an anion vacancy against thermal annihilation.

At 1100 K, [H<sup>-</sup>]<sup>+</sup> centers ultimately are annihilated [Fig. 5(f)]. Annealing at 1000 and 1100 K resulted in a broad 5.3 eV band (Fig. 4). This band has previously been observed in MgO:Li crystals annealed at temperatures above 1400 K, regardless of the ambient atmosphere. This band is charac-

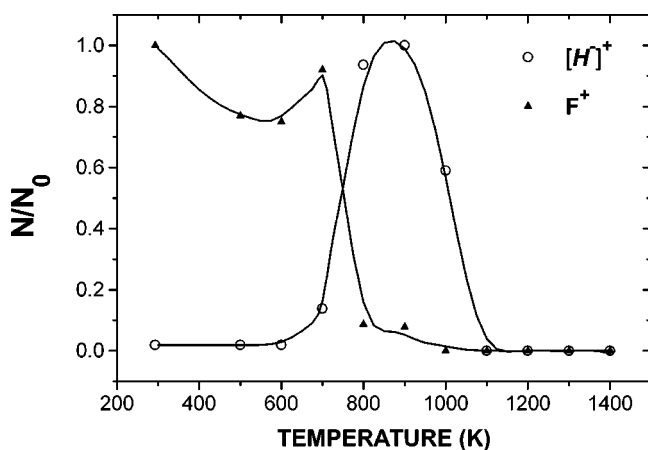


FIG. 6. Normalized concentration of  $F^+$  and  $[H^-]^+$  centers vs isochronal annealing temperature of the MgO:Li crystal used in Figs. 4 and 5.

teristic of MgO:Li only and has not been observed in MgO crystals not doped with lithium impurities. The defect responsible for this band appear to be diamagnetic and therefore its structure has not been identified; it is likely related to the association of substitutional lithium ions and oxygen vacancies.<sup>28</sup> Annealing at 1200 K essentially returned the crystal to its preirradiation state [Figs. 4 and 5(g)].

The behavior of the  $F^+$  and  $[H^-]^+$  bands during the thermal anneals is summarized in Fig. 6. Clearly,  $[H^-]^+$  centers are not formed in significant concentrations until the temperature is sufficiently high for protons in microcavities and  $\text{OH}^-$  configurations to become mobile and diffuse into the oxygen vacancies. This proton activity begins to occur at about 700 K. Proton occupation renders the vacancy more stable against thermal annihilation, in agreement with previous findings.<sup>24</sup>

The results of Fig. 3 suggest that most of the  $\text{Li}^+$  substitutional ions were displaced from their sites during irradiation and relocated somewhere else. However, this process is reversible: thermal anneals at sufficiently high temperatures not only destroy  $F^+$  and  $[H^-]^+$  centers, but also disperse  $\text{Li}^+$  ions, and the broad  $\text{OH}^-$  absorption band is restored [Fig. 5(g)]. Both protons and lithium ions become mobile at temperatures of about 700 and 1100 K, respectively (Fig. 5). The latter temperature coincides with that found earlier for the dispersion of  $\text{Li}^+$  ions from  $\text{Li}_2\text{O}$  precipitates during oxidation of as-grown MgO:Li crystals.<sup>29</sup> We postulate that the irradiation-displaced ions likely form  $\text{Li}_2\text{O}$  precipitates. Our speculation is based on the following observations: (1) the concentration of thermally generated  $[\text{Li}]^0$  centers in MgO:Li crystals was observed to decrease upon neutron irradiation<sup>25</sup>; (2) after thermal anneals of neutron-irradiated MgO:Li, the IR spectra in Fig. 5 show that the broadband at  $3430\text{ cm}^{-1}$  (associated with  $\text{OH}^-$  complexes perturbed by  $\text{Li}^+$  ions) is restored at the same temperature  $[\text{Li}]^0$  centers are formed at the expense of  $\text{Li}^+$  ions from  $\text{Li}_2\text{O}$  precipitates, during oxidation of as-grown MgO:Li crystals<sup>29</sup>; and (3) a parallelism in the behavior of  $\text{Li}^+$  and  $\text{H}^+$  ions under ionizing radiation in MgO:Li and in lithium-free MgO crys-

tals containing hydrogen: both light ions form  $\text{Li}_2\text{O}$  and  $\text{Mg}(\text{OH})_2$  precipitates, respectively.

#### IV. DISCUSSION

We shall first address the effect of irradiation on protons in MgO:H crystals. Hydrogen is normally present in three forms: (a) high-pressure hydrogen gas in microcavities,<sup>18,19</sup> (b) protons substituting for magnesium ions, forming  $V_{\text{OH}}^-$  centers,<sup>21,22</sup> and (c)  $\text{Mg}(\text{OH})_2$  (brucite) precipitates.<sup>21,22</sup> Infrared absorption spectroscopy identifies the protons, or  $\text{OH}^-$  ions, in both the substitutional and precipitate forms. The distribution of protons between the two forms depends on the past thermal history of the sample, notably the cooling rate. Slow cooling favors the precipitates, while quenching favors the substitutional form.<sup>11</sup> During irradiation, protons are displaced by an ionization process, with a phenomenally large cross section of  $10^8\text{ b}$ . Therefore in a reactor, it is the Compton electrons, due to the attending gamma rays, that cause the displacement of protons. The displaced protons find themselves forming  $\text{Mg}(\text{OH})_2$  precipitates, leaving behind magnesium vacancies in the form of  $V^-$  centers.<sup>12</sup> The latter has been identified by electron paramagnetic resonance (EPR).

In contrast, our understanding of the MgO:Li system is nowhere as thorough, simply because of the lack of a spectroscopic tool to monitor lithium ions. Nevertheless, the results of the present study permit us to draw some conclusions about the fate of the lithium ions during irradiation. Lithium impurities are present<sup>30,31</sup> in three forms: (a) an isolated  $\text{Li}^+$  ion substituting for a  $\text{Mg}^{2+}$  ion and therefore negatively charged with respect to its surroundings. EPR has identified the substitutional  $\text{Li}^+$  ion when it has trapped a hole at low temperatures. This hole is unstable at room temperature. (b) A  $\text{Li}^+$  ion nearby an  $\text{OH}^-$  ion. This complex gives rise to the broad absorption band at  $3430\text{ cm}^{-1}$  without sharp features. The fact that this band is characteristic of lithium doping indicates that it is due to  $\text{OH}^-$  ions perturbed by lithium ions. Lithium has a strong affinity for hydrogen. While it is possible to grow MgO crystals with a minimal amount of protons, it has not been possible to dope them with lithium without a large amount of hydrogen. In this sense, the presence of protons complicates the problem, but at the same time permits the use of infrared spectroscopy to monitor the  $\text{Li}^+$  ions indirectly. (c)  $\text{Li}_2\text{O}$  precipitates, identifiable by transmission electron microscopy.<sup>31</sup>

Given, from previous studies,<sup>12,24</sup> that the cross sections of displacements are  $10^8$  and  $10^5\text{ b}$  for protons and  $\text{Li}^+$  ions, respectively, the displacements of these two light impurities readily takes place by ionizing Compton electrons— independent of the displacement of the anions by elastic collisions with neutrons. While there is an abundance of hydrogen in the crystal, no  $\text{Mg}(\text{OH})_2$  precipitates have been observed in lithium-doped crystals, regardless of heat treatment. This observation suggests that the presence of lithium prevents the formation of brucite precipitates. During reactor irradiation protons are the first to be displaced, followed by  $\text{Li}^+$  ions. Therefore we postulate that the displaced protons have nowhere to go and eventually end up where they

started. Next, the isolated  $\text{Li}^+$  ions are displaced, leaving behind cation vacancies. These vacancies are quickly occupied by the rampant protons, giving rise to the  $V_{OH}^-$  centers, as noted by the  $3296\text{ cm}^{-1}$  band, shown in Figs. 3(b)–3(d). The displaced  $\text{Li}^+$  ions cannot return to their original sites, because they are already occupied by the more mobile protons.  $\text{Li}^+$  ions from the adjacent  $\text{OH}^-$  complex are likewise displaced, resulting in a decrease of the  $3430\text{ cm}^{-1}$  band. We also postulate that the displaced  $\text{Li}^+$  ions contribute to  $\text{Li}_2\text{O}$  precipitates, either by enlarging old ones or forming new ones. At some later point, ample anion vacancies are formed by the neutron bombardment. These vacancies can readily capture protons, giving rise to the  $[\text{H}^-]^+$  band at  $1024\text{ cm}^{-1}$  [Fig. 3(b)], and just as readily lose them by ionizing radiation to other configurations, such as the  $V_{OH}^-$  centers [Figs. 3(c) and 3(d)].

Annealing experiments permit us to explore the reverse process of radiation-induced defect formation and provide us with information on the thermal activities of the light ions. We know from previous works<sup>12,29</sup> that protons and  $\text{Li}^+$  ions are mobile at 700 K and 1100 K, respectively. In the present study on a  $\text{MgO}:\text{Li}$  crystal irradiated to  $10^{19}$  neutrons/ $\text{cm}^2$ , we observed that (a) protons from  $V_{OH}^-$  centers and the microcavities began to be thermally active at 700 K and occupy anion vacancies giving rise to the  $[\text{H}^-]^+$  centers at  $1024\text{ cm}^{-1}$ , as shown in Fig. 5(b); and (b)  $\text{Li}^+$  ions which had been displaced from the lithium-perturbed  $\text{OH}^-$  ions returned at 1100 K to give rise to the broad  $3430\text{ cm}^{-1}$  band again [Fig. 5(f)]. Therefore the formation and destruction of radiation-induced defects involving  $\text{H}^+$  and  $\text{Li}^+$  are consistent with the temperatures at which these light impurities are known to be thermally active.

## V. SUMMARY AND CONCLUSIONS

The radiation damage induced by neutron irradiation in the dose range  $10^{15}$ – $10^{19}$  neutrons/ $\text{cm}^2$  was studied in nominally pure, hydrogen-doped, and lithium-doped  $\text{MgO}$  crys-

tals. The conclusions derived are the following.

(1) The present work confirms that the concentrations of anion vacancies and higher-order point defects increases with neutron dose.

(2) This work also confirms that high concentrations of hydrogen, in the form of high-pressure hydrogen gas inside microcavities, suppress the formation of anion vacancies and higher-order defects. These microcavities serve as a sink for migrating vacancies. A net reduction of 35% anion-vacancy concentrations has been observed.

(3) In lithium-doped crystals (which have a strong affinity for hydrogen) irradiated with neutron doses below  $10^{18}$  neutrons/ $\text{cm}^2$ , the diminished concentration of anion vacancies and higher-order defects is camouflaged by the occupancy of these vacancies by protons, giving rise to hydride or  $[\text{H}^-]^+$  ions. The ratio of the concentration of  $[\text{H}^-]^+$  ions to anion vacancies was observed to be more than 2:1.

(4) Lithium ions are displaced from the isolated sites, leaving behind cation vacancies which quickly capture protons to form  $V_{OH}^-$  ions. Likewise, lithium ions are displaced from the  $\text{OH}^-$  complex, resulting in a decrease of the  $3430\text{ cm}^{-1}$  band. It is postulated that the displaced lithium ions form  $\text{Li}_2\text{O}$  precipitates.

(5) Thermal annealing experiments demonstrate that protons are mobile at 700 K and lithium ions at 1100 K, consistent with what is known of the mobilities of these light-ion impurities.

## ACKNOWLEDGMENTS

Research at the University Carlos III was supported by the CICYT of Spain. The research of Y.C. is an outgrowth of past investigations performed at the Solid State Division of the Oak Ridge National Laboratory. The irradiation at the High Flux Reactor of the Institute for Advanced Materials of the Joint Research Center (JRC) at Petten was carried out under Contract No. 40.00024 with the European Atomic Energy Commission.

- 
- <sup>1</sup>M.A. Monge, A.I. Popov, C. Ballesteros, R. González, Y. Chen, and E.A. Kotomin, *Phys. Rev. B* **62**, 9299 (2000).  
<sup>2</sup>Y. Chen, J.L. Kolopus, and W.A. Sibley, *Phys. Rev.* **25**, 2077 (1969).  
<sup>3</sup>L.A. Kappers, R.L. Kroes, and E.B. Hensley, *Phys. Rev. B* **1**, 4151 (1970).  
<sup>4</sup>I.K. Ludlow and W.A. Runciman, *Proc. Phys. Soc. London* **86**, 1081 (1965).  
<sup>5</sup>I.K. Ludlow, *Proc. Phys. Soc. London* **88**, 763 (1966).  
<sup>6</sup>B. Henderson and J.E. Wertz, *Adv. Phys.* **17**, 749 (1968).  
<sup>7</sup>Y. Chen, R.T. Williams, and W.A. Sibley, *Phys. Rev.* **182**, 960 (1969).  
<sup>8</sup>B. Henderson and R.D. King, *Philos. Mag.* **13**, 1149 (1966).  
<sup>9</sup>Y. Chen and W.A. Sibley, *Philos. Mag.* **20**, 217 (1969).  
<sup>10</sup>R. González, Y. Chen, R.M. Sebeck, G.P. Williams, Jr., R.T. Williams, and W. Gellermann, *Phys. Rev. B* **43**, 5228 (1991).  
<sup>11</sup>Y. Chen, M.M. Abraham, L.C. Templeton, and W.P. Unruh, *Phys. Rev. B* **11**, 881 (1975).  
<sup>12</sup>Y. Chen, M.M. Abraham, and H.T. Tohver, *Phys. Rev. Lett.* **37**, 1757 (1976).  
<sup>13</sup>W.A. Sibley and Y. Chen, *Phys. Rev.* **160**, 712 (1967).  
<sup>14</sup>B. Henderson, D.H. Bowen, A. Briggs, and R.D. King, *J. Phys. C* **4**, 1496 (1971).  
<sup>15</sup>Y. Chen and M.M. Abraham, *J. Am. Ceram. Soc.* **59**, 101 (1976).  
<sup>16</sup>M.M. Abraham, C.T. Butler, and Y. Chen, *J. Chem. Phys.* **55**, 3752 (1971).  
<sup>17</sup>Y. Chen, D.L. Trueblood, O.E. Schow, and H.T. Tohver, *J. Phys. C* **3**, 2501 (1970).  
<sup>18</sup>A. Briggs, *J. Mater. Sci.* **10**, 729 (1975).  
<sup>19</sup>M.S. Corisco, R. González, and C. Ballesteros, *Philos. Mag. A* **52**, 699 (1985).  
<sup>20</sup>B. Henderson and D.H. Bowen, *J. Phys. C* **4**, 1487 (1971).

- <sup>21</sup>B. Henderson and W.A. Sibley, *J. Chem. Phys.* **55**, 1276 (1971).
- <sup>22</sup>B. Henderson, J.L. Kolopus, and W.P. Unruh, *J. Chem. Phys.* **55**, 3518 (1971).
- <sup>23</sup>R. González, Y. Chen, and M. Mostoller, *Phys. Rev. B* **24**, 6862 (1981).
- <sup>24</sup>R. González, R. Pareja, and Y. Chen, *Phys. Rev. B* **45**, 12 730 (1992).
- <sup>25</sup>Y. Chen, E. Montesa, J.L. Boldú, and M.M. Abraham, *Phys. Rev. B* **24**, 5 (1981).
- <sup>26</sup>R. González, Y. Chen, and K.L. Tsang, *Phys. Rev. B* **26**, 4637 (1982).
- <sup>27</sup>Y. Chen, R. González, O.E. Schow, and G.P. Summers, *Phys. Rev. B* **27**, 1276 (1983).
- <sup>28</sup>V.M. Orera, Y. Chen, and M.M. Abraham, *Philos. Mag. A* **41**, 431 (1980).
- <sup>29</sup>M.M. Abraham, Y. Chen, L.A. Boatner, and R.W. Reynolds, *Phys. Rev. Lett.* **37**, 849 (1976).
- <sup>30</sup>J. Narayan, M.M. Abraham, Y. Chen, and H.T. Tohver, *Philos. Mag. A* **38**, 247 (1978).
- <sup>31</sup>J.B. Lacy, M.M. Abraham, J.L. Boldú, Y. Chen, J. Narayan, and H.T. Tohver, *Phys. Rev. B* **18**, 4136 (1978).